

# Nano Effects of Nitrogen Ion Implantation on TiN Hard Coatings Deposited by PVD and IBAD

Branko Skoric, Aleksandar Miletic, Pal Terek, Lazar Kovacevic, Milan Kukuruzovic

**Abstract**—In this paper, we present the results of a study of TiN thin films which are deposited by a Physical Vapour Deposition (PVD) and Ion Beam Assisted Deposition (IBAD). In the present investigation the subsequent ion implantation was provided with  $N^{5+}$  ions. The ion implantation was applied to enhance the mechanical properties of surface. The thin film deposition process exerts a number of effects such as crystallographic orientation, morphology, topography, densification of the films. A variety of analytic techniques were used for characterization, such as scratch test, calo test, Scanning electron microscopy (SEM), Atomic Force Microscope (AFM), X-ray diffraction (XRD) and Energy Dispersive X-ray analysis (EDAX).

**Keywords**—Steel, coating, super hard, ion implantation, nanohardness.

## I. INTRODUCTION

THE evolution of the microstructure from porous and columnar grains to dense packed grains is accompanied by changes in mechanical and physical properties. Ion implantation has the capabilities of producing new compositions and structures unattainable by conventional means. Implantation may result in changes in the surface properties of a material, including hardness, wear, coefficient of friction and other properties.

The optimization procedure for coated parts could be more effective, knowing more about the fundamental physical and mechanical properties of a coating. In this research are present the results of a study of the relationship between the process, composition, microstructure and nanohardness of duplex TiN coatings and modified with ion implantation.

A duplex surface treatment involves the sequential application of two surface technologies to produce a surface composition with combined properties [1]. A typical duplex process involves plasma nitriding and the coating treatment of materials. The duplex coating method can improve further of the tribological properties and load-bearing capacity of materials beyond metals. The synthesis of the TiN film by IBAD has been performed by irradiation of Ar ions. Ion implantation has the capabilities of producing new compositions and structures unattainable by conventional means.

Thin hard coatings deposited by physical vapor deposition (PVD), e.g. titanium nitride (TiN) are frequently used to improve tribological performance in many engineering

applications [2]. In many cases single coating cannot solve the wear problems [3]. The combination of nitriding and hard coating allows the production of duplex coatings, which are distinguished by a high resistance against complex loads, since the advantages of both individual processes are combined here. The effects on the structure as well as mechanical and tribological properties of the films were investigated in detail in the present research.

The results were correlated with properties determined from mechanical and tribological characterization. Therefore, by properly selecting the processing parameters, well-adherent TiN films with low friction coefficient, low wear rate and high hardness can be obtained on engineering steel substrates, and show a potential for tribological applications.

The duplex surface treatment was used to enhance adhesion strength and hardness of hard coatings.

The depth of nanopenetration provides an indirect measure of the area of contact at full load and thus hardness is obtained by dividing the maximum applied load with the contact area. Micro hardness testing, Vickers micro hardness, is dependent on visual resolution of the residual indent for accurate measurement. The diagonal of the indent, which is the key for hardness determination, is sometimes very hard to resolve if the load is low enough to avoid cracking and again this would be much more difficult if cracking occurs at high load within the indent site.

In the nanoindentation technique, hardness and Young's modulus can be determined by the Oliver and Pharr method [4], where hardness ( $H$ ) can be defined as:  $H = \frac{P_{max}}{A}$ , where  $P_{max}$

is maximum applied load, and  $A$  is contact area at maximum load. In nanoindentation, the Young's Modulus,  $E$ , can be obtained from:

$$\frac{1}{E_r} = \frac{1-\nu^2}{E} + \frac{1-\nu_i^2}{E_i} \quad (1)$$

where  $\nu_i$ =Poisson ratio of the diamond indenter (0.07) and  $E_i$ =Young's modulus of the diamond indenter.

Therefore, in recent years, a number of measurements have been made in which nanoindentation and AFM have been combined.

## II. EXPERIMENTAL

The substrate material used was high speed steel type S 6-5-2. Prior to deposition the substrate was mechanically polished to a surface roughness of  $0.12 \mu m$  ( $R_a$ ). The specimens were

Branko Skoric is with the University of Novi Sad, Faculty of Technical Sciences, Center for Surface Engineering and Nanotechnology, 21000 Novi Sad, Serbia (e-mail: skoricb@uns.ac.rs)

first austenized, quenched and then tempered to the final hardness of 850 HV. In order to produce good adhesion of the coating, the substrates were plasma nitrided at low pressure ( $1 \times 10^{-3}$  Pa), prior to deposition of the coating. The PVD treatment was performed in a Balzers Sputron installation with rotating specimen. The gas flow into the deposition chamber was controlled by mass flow meters and the partial pressures of argon and nitrogen were measured. The deposition parameters were as follows: Base pressure in the chamber was  $1 \times 10^{-5}$  mbar, bias voltage  $U_b=1$  kV, discharge current  $I_d=50$  mA, substrate temperature  $T_s=200$  °C, target to substrate distance  $d_{s-t}=120$  mm. The partial pressure of Ar during deposition was  $P_{Ar}=(3.1-6.6) \times 10^{-6}$  mbar and partial pressure of  $N_2$  was  $P_{N_2}=6.0 \times 10^{-6}-1.1 \times 10^{-5}$  mbar. Deposition rate  $a_D=0.1$  nm/s. Prior to entering the deposition chamber the substrates were cleaned.

Other samples were produced with IBAD technology in DANFYSIK chamber. The IBAD system consists of an e-beam evaporation source for evaporating Ti metal and 5-cm-diameter Kaufman ion source for providing argon ion beam. Base pressure in the IBAD chamber was  $1 \times 10^{-6}$  mbar. The partial pressure of Ar during deposition was  $(3.1-6.6) \times 10^{-6}$  mbar and partial pressure of  $N_2$  was  $6.0 \times 10^{-6}-1.1 \times 10^{-5}$  mbar. The ion energy ( $E_{Ar}=1.5-2$  keV), ion beam incident angle ( $15^\circ$ ), target to substrate distance  $d_{s-t}=360$  mm, and substrate temperature  $T_s=200$  °C, were chosen as the processing variables. Deposition rate  $a_D=0.05-0.25$  nm/s. Quartz crystal monitor was used to gauge the approximate thickness of the film. Additional analyze the thickness of coatings, the ball crater method (calo-test), allows prompt and sufficiently precise results to be obtained.

A pure titanium intermediate layer with a thickness of about 50nm has been deposited first for all the coatings to enhance the interfacial adhesion to the substrates. After deposition, the samples were irradiated with 120 keV,  $N^{5+}$  ions at room temperature (RT). The Ion Source is a multiply charged heavy ion injector, based on the electron cyclotron resonance effect (ECR). The implanted fluencies were in the range from  $0.6 \times 10^{17}$  to  $1 \times 10^{17}$  ions/cm<sup>2</sup>.

The mechanical properties on coated samples were characterized using a Nanohardness Tester (NHT) developed by CSM Instruments, Switzerland. Nanoindentation testing was carried out with applied loads in the range of 10 to 20 mN. The nanohardness tester was calibrated by using fused silica samples for a range of operating conditions. A Berkovich diamond indenter was used for all the measurements. The tip radius of the indenter was approximately 50 nm and the displacement resolution of the machine was 0.03 nm. The data was processed using proprietary software to produce load-displacement curves and the mechanical properties were calculated using the Oliver and Pharr method. At least ten measurements were made at each load on the coated sample. Measurement of hardness was also carried out using a conventional Vickers microhardness tester. The Nano-Hardness tester uses an already established method where a

Berkovich indenter tip with a known geometry is driven into a specific site of the material to be tested, by applying an increasing normal load. For each loading/unloading cycle, the applied load value is plotted with respect to the corresponding position of the indenter. The maximum indentation depth for measuring H and E was fixed at one tenth of the coating thickness.

The analysis of the indents was performed by Atomic Force Microscope (AFM). The analyzed AE signal was obtained by a scratching test designed for adherence evaluation. Scratch tests were performed under controlled conditions with a device that consisted of a loaded probe with a diamond indenter moving linearly along the sample with a constant speed and continuously increasing force. The steadily increasing contact load causes tensile stress behind the indenter tip and compressive stress ahead of the cutting tip. Detection of elastic waves generated as a result of the formation and propagation of microcracks. The AE sensor is insensitive to mechanical vibration frequencies of the instrument. This enables the force fluctuations along the scratch length to be followed, and the friction coefficient to be measured. The scratch tester equipment with an acoustic sensor (CSM-REVETEST) was used.

X-ray diffraction studies were undertaken in an attempt to determine the phases present, and perhaps an estimate of grain size from line broadening. The determination of phases was realized by X-ray diffraction using PHILIPS APD 1700 X-ray diffractometer. The X-ray sources were from  $CuK_\alpha$  with wavelength of 15.443 nm (40 kV, 40 mA) at speed 0.9°/min. The surface roughness was measured using stylus type (Talysurf Taylor Hobson) instruments. The most popular experimental XRD approach to the evaluation of residual stresses in polycrystalline materials is the  $\sin^2\psi$  method. For each selected (hkl) crystallographic direction, diffraction data are collected at different  $\psi$  tilting angles. The method requires a  $\theta$ - $2\theta$  scan for every  $\psi$  angle around the selected diffraction peak and, in order to emphasize the peak shifts, it is important to work at the highest possible  $2\theta$  angle.

### III.RESULTS

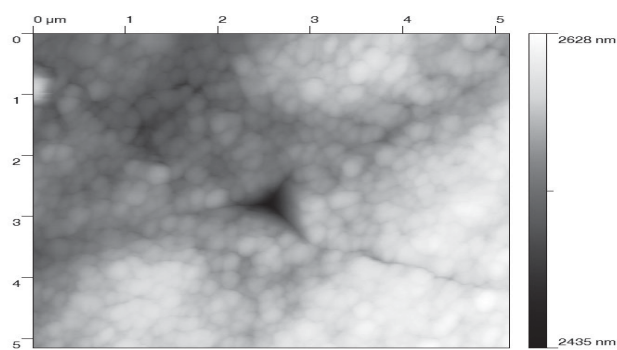
The nitrogen to metal ratio, EDX, Table I, is stoichiometries for IBAD technology and something smaller from PVD. For sample with additional ion implantation, value is significantly different, smaller. It is possibly diffused from the layer of TiN to the interface. The TiN coatings only show a golden surface and after ion implantation the color is dark golden

TABLE I  
ATOMIC RATIO N/Ti IN COATING

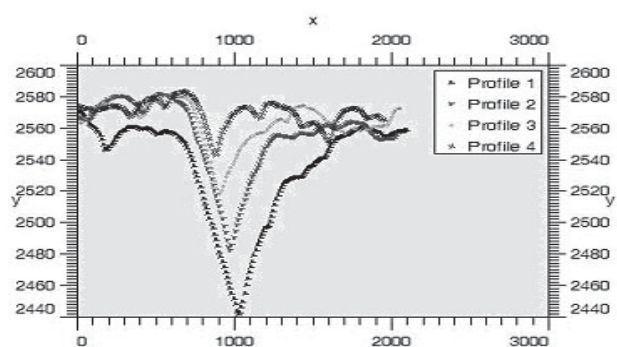
	Coating	Ratio N/Ti (atomic)
1	IBAD	1.00
2	PVD	0.98
3	PVD/III	0.89

The analysis of the indents was performed by Atomic Force Microscope (Fig. 1 (a)). It can be seen, from cross section of

an indent during indentation, that the indents are regularly shaped with the slightly concave edges typically seen where is significant degree of elastic recovery (Fig. 1 (b)).



(a)



(b)

Fig. 1 (a) AFM image of a nanoindentation and (b) Cross-section of the indentation

All the results of nanohardness are obtained with the Oliver & Pharr method and using a supposed sample Poisson's ratio of 0.3 for modulus calculation.

The nanohardness values and microhardness are shown in Table II.

For each measurement, the penetration (Pd), the residual penetration (Rd), the acoustic emission (AE) and the frictional force are recorded versus the normal load. The breakdown of the coatings was determined both by AE signal analysis and optical and scanning electron microscopy.

TABLE II  
SURFACE MICROHARDNESS (HV0.03) AND NANOHARDNESS (LOAD-10mN)

Unit	pn/IBAD	PVD	pn/PVD/II	Fused Silica
Vickers	2007	3028	3927	943
GPa	21.6	32.6	42.6	10.1

TABLE III  
CRITICAL LOAD FOR DIFFERENT TYPE OF COATING

	pn/TiN(IBAD)	pn/TiN(PVD)
Lc1	-	23
Lc2	100	54
Lc3	138	108

AE permits an earlier detection, because the shear stress is a maximum at certain depth beneath the surface, where a subsurface crack starts. Critical loads are presents in Table III.

The critical load Lc1 corresponds to the load inducing the first crack on the coating. No cracks were observed on sample 1. The critical load Lc2 corresponds to the load inducing the partial delamination of the coating. The critical load Lc3 corresponds to the load inducing the full delamination of the coating. AE permits an earlier detection, because the shear stress is a maximum at certain depth beneath the surface, where a subsurface crack starts (PVD), Fig. 2.

It was found that the plasma-nitriding process enhanced the coating to substrates adhesion. In some places of hard coatings cohesive failure of the coating and the delamination of the coating was observed (Fig. 3).

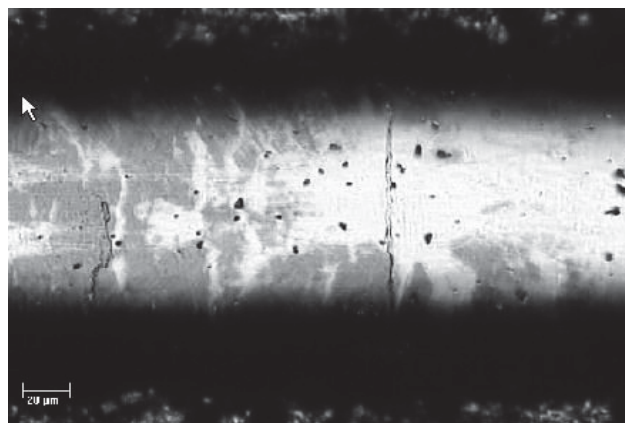


Fig. 2 Partial delamination of coating

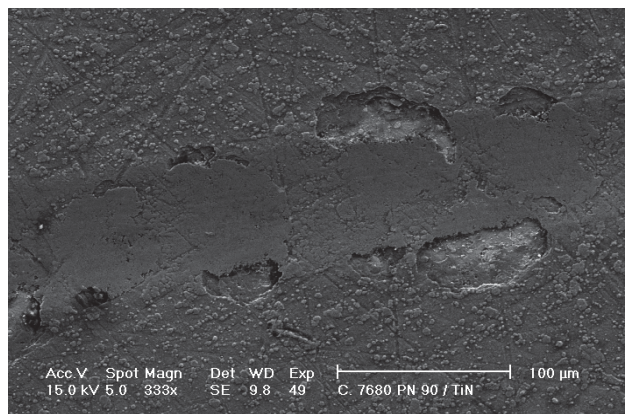


Fig. 3 SEM morphology of scratch test: pn/TiN(PVD)

The nanoindentation elastic modulus was calculated using the Oliver-Pharr data analysis procedure. The individual values of E are the different for all measurements, Fig. 4.

The errors related to the measurements and estimations were different and for duplex coating with ion implantation is less than 4%. Good agreement could be achieved between the  $E_c$  values and nanohardness.

The tribological behaviour of the coatings was studied also by means of pin-on-ring contact configuration in dry sliding conditions, described elsewhere [5].

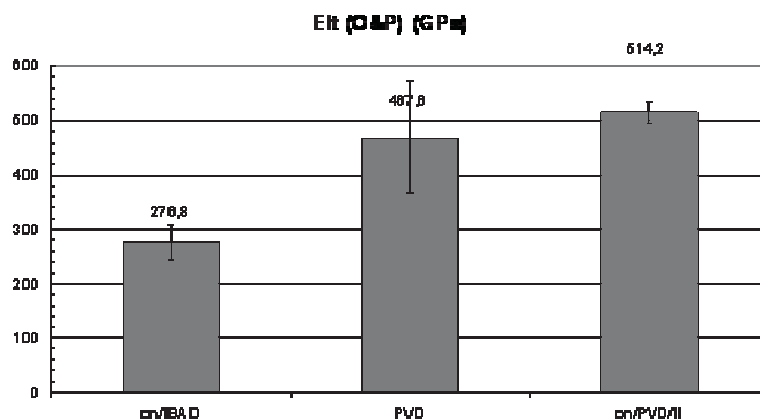


Fig. 4 Young's elastic module

The stress determination follows the conventional  $\sin^2\psi$  method. Stress determination was performed using a PHILIPS XPert diffractometer. The (422) diffraction peak was recorded in a  $2\theta$  interval between  $118^\circ$  and  $130^\circ$ , with tilting angle:  $\psi_0^1=0^\circ$ ,  $\psi_0^2=18.75^\circ$ ,  $\psi_0^3=27.03^\circ$ ,  $\psi_0^4=33.83^\circ$ ,  $\psi_0^5=40^\circ$ . A typical result for compact film, with residual stresses  $\sigma = -4.28\text{GPa}$ , has TiN(PVD).

Coating is often in tensile stress with greater microhardness. The (422) diffraction peak was recorded in a  $2\theta$  interval between  $118^\circ$  and  $130^\circ$ , with tilting angle. A typical result for compact film, with residual stresses  $\sigma = -4.28\text{GPa}$ , has TiN(PVD), is shown in Fig. 5.

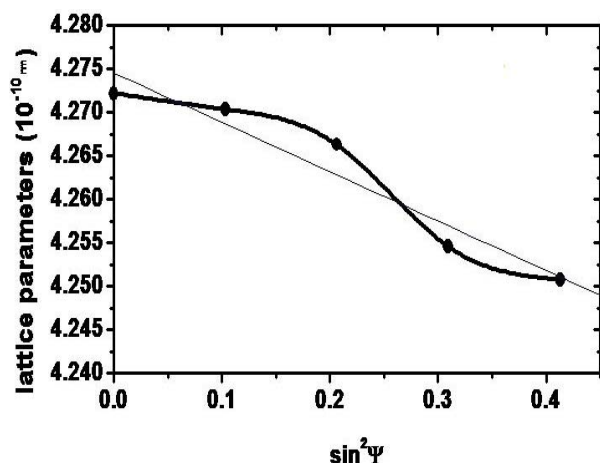


Fig. 5 The  $a(hkl)$  vs.  $\sin^2\psi$  plots

In the case shear stress results in splitting in  $d$  vs.  $\sin^2\psi$ , for  $+\psi$  and  $-\psi$ . The simplest form of X-ray diffraction (XRD) characterization of thin film microstructure is Cohen-Wagner plot, Fig. 6.

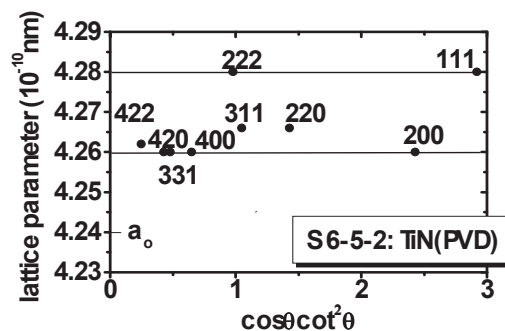


Fig. 6 The Cohen-Wagner plot, lattice parameters  $a_{hkl}$  vs.  $\cos\theta \cos^2\theta$

The anisotropy of lattice parameters,  $a_{hhh} \gg a_{hoo}$ , is characteristic for compact film. The coating morphology was evaluated using the well-known structure zone model of Thornton. All observed morphologies are believed to be from region of zone I (PVD) and from the border of region zone T (IBAD). It has been suggested, that the transition from open porous coatings with low microhardness and rough surface, often in tensile stress to dense coatings films with greater microhardness, smooth surface occurs at a well defined critical energy delivered to the growing film.

#### IV. DISCUSSIONS

A hardness increase is observed for implanted samples. This can be attributed to iron nitride formation in the near surface regions. The standard deviation of the results is relatively important due to the surface roughness of the samples. Because the thickness of the TiN coatings presented here is sufficiently large, which for all coatings is about 2900 nm (TiN-PVD), the hardness measurements will not be affected by the substrate, as in three times thinner (900 nm TiN-IBAD).

The individual values of  $E$  are the different for all measurements. The errors related to the measurements and estimations were different and for duplex coating with ion



implantation is less than 4%. Good agreement could be achieved between the  $E_c$  values and nanohardness.

The wear resistance of the TiN coating was obviously improved by the presence of a nitride interlayer. Such an

improvement is probably due to the adequate bonding between the nitrided layer and substrate. SEM micrograph of wear track showed that the transfer layer consists of small amount of counter material (adhesive wear), Fig. 7.

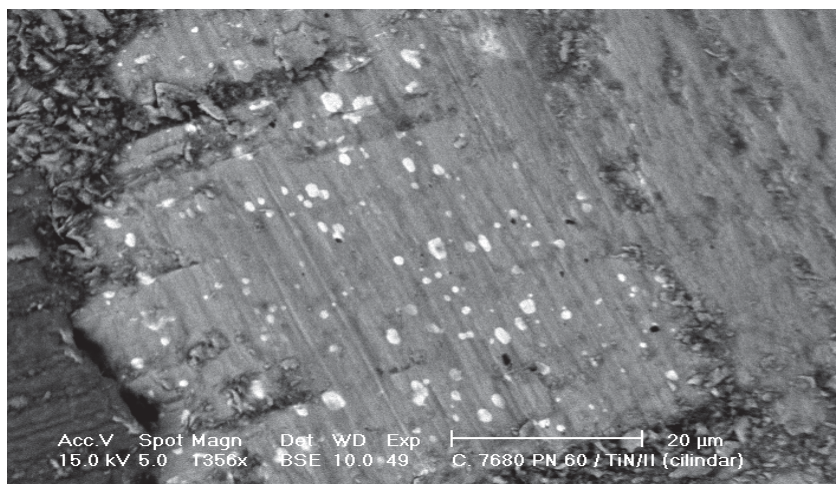


Fig. 7 SEM micrograph of wear track (BSE), with wear debris

It is generally expected that an increase in hardness results in an increase in wear resistance.

The PVD coating process did not significantly change roughness. For the practical applications of IBAD coatings, it is important to know that the roughness of the surface decreased slightly after deposition (from  $R_a=0.19\ \mu\text{m}$  to  $R_a=0.12\ \mu\text{m}$ ).

The formation of TiN by IBAD has its origin in a kinetically controlled growth. The nitrogen atoms occupy the octahedric sites in varying number according to the energy that these atoms possess to cross the potential barriers created by the surrounding titanium anions. The ion bombardment is believed to enhance the mobility of the atoms on the sample surface. XRD analysis revealed the presence of only one phase,  $\delta$ -TiN, and there is no evidence for other phases, such as  $\text{Ti}_2\text{N}$ , could be found. The  $\varepsilon$ - $\text{Ti}_2\text{N}$  does not lead to an improvement in the tribological behavior.

The coating morphology was evaluated using the well-known structure zone model of Thornton. All observed morphologies, are believed to be from region of zone I (PVD) and from the border of region zone T (IBAD). It has been suggested [6], that the transition from open porous coatings with low microhardness and rough surface, often in tensile stress to dense coatings films with greater microhardness, smooth surface occurs at a well defined critical energy delivered to the growing film.

#### V.CONCLUSIONS

The experimental results indicated that the mechanical hardness is elevated by penetration of nitrogen, whereas the Young's modulus is significantly elevated. Nitrogen ion

implantation leads to the formation of a highly wear resistant and hard surface layer.

The deposition process and the resulting coating properties depend strongly on the additional ion bombardment.

Nitrogen implantation into hard TiN coatings increases the surface hardness and significantly reduces the tendency of the coatings to form microcracks when subjected to loads or stresses.

Nitrogen implantation into hard TiN coatings increases the surface hardness and significantly reduces the tendency of the coatings to form microcracks when subjected to loads or stresses.

The above findings show that deposition process and the resulting coating properties depend strongly on the additional ion bombardment.

#### ACKNOWLEDGMENT

The authors gratefully acknowledge the financial support from the Ministry of Education, Science and Technological Development of the Republic of Serbia and Provincial Secretariat for Science and Technological Development of Vojvodina.

#### REFERENCES

- [1] J.C.A. Batista, C. Godoy and A. Matthews A. Leyland, "Developments Towards Producing Well Adherent Duplex PAPVD Coatings", *Surface Engineering*, 9, 37-43.,2003.
- [2] Y. Sun and T. Bell, "Plasma surface engineering of low alloy steel" I, *Mater. Sci. Eng., A* 140, 419-434.,1991.
- [3] H. Haufmann, "Industrial applications of plasma and ion surface engineering" *Surface and Coatings Technology*, 74-75, 23-28. 1988.
- [4] Pharr, G.M., Oliver, W.C., Brotzen, F.R., "On the generality of the relationship among contact stiffness, contact area, and elastic modulus during indentation", *J. Mater. Res.*, 7, 613.,1992.

- [5] B. Škorić and D. Kakaš, "Influence of plasma nitriding on mechanical and tribological properties of steel with subsequent PVD surface treatments", *Thin Solid Films*, 317, 486-489.,1998.
- [6] L. Combadiere, J. Machet, "Reactive magnetron sputtering deposition of TiN films", *Surface and Coating Technology*, 88, 17-27.,1996.